Annealing effect on the optical properties of implanted silicon in a silicon nitride matrix

Fung, Stevenson Hon Yuen; Liu, Yang; Yang, Ming; Wong, Jen It; Liu, Yu Chan; Liu, Zhen; Cen, Zhan Hong; Chen, Tupei; Ding, Liang

2008

Cen, Z. H., Chen, T., Ding, L., Liu, Y., Yang, M., Wong, J. I., et al. (2008). Annealing effect on the optical properties of implanted silicon in a silicon nitride matrix. Applied Physics Letters, 93, 1-3.

https://hdl.handle.net/10356/101981

https://doi.org/10.1063/1.2962989

Annealing effect on the optical properties of implanted silicon in a silicon nitride matrix

Z. H. Cen,[1,a)] T. P. Chen,[1,b)] L. Ding,[1] Y. Liu, M. Yang,[1] J. I. Wong,[1] Z. Liu,[1] Y. C. Liu,[2] and S. Fung[3]
[1]*School of Electrical and Electronic Engineering, Nanyang Technological University, Singapore 639798, Singapore*
[2]*Singapore Institute of Manufacturing Technology, Singapore 638075, Singapore*
[3]*Department of Physics, The University of Hong Kong, Hong Kong, People's Republic of China*

(Received 16 January 2008; accepted 30 June 2008; published online 17 July 2008)

Optical properties of implanted Si in a silicon nitride (Si_3N_4) thin film have been determined with spectroscopic ellipsometry based on the Tauc–Lorentz (TL) model and the Bruggeman effective medium approximation. It is shown that the suppressed dielectric functions of the implanted Si are dominated by the energy transitions related to the critical point E_2. The effect of thermal annealing on the dielectric functions of the implanted Si has been investigated. The analysis of the dielectric functions based on the evolution of the TL parameters can provide an insight into the structural changes in the implanted Si embedded in the Si_3N_4 matrix caused by the annealing. © *2008 American Institute of Physics*. [DOI: 10.1063/1.2962989]

Recently, the silicon-rich silicon nitride (Si_3N_4) systems that offer advantages of stronger light emission and lower barrier height for carrier injection compared with those of SiO_2,[1–3] have attracted a lot of attentions. One of the techniques that can be used to synthesize the silicon-rich Si_3N_4 is Si ion implantation into a Si_3N_4 thin film. In the present work, spectroscopic ellipsometry (SE) is used to determine the optical properties of the silicon implanted in the Si_3N_4 matrix, and the effect of postimplant thermal annealing on the optical properties is studied. Such a study is obviously important to the fundamental physics and the technological applications as well.

A multilayer optical model[4,5] together with the Bruggeman effective medium approximation[6] (BEMA) has been employed to analyze the SE response of the Si_3N_4 thin film implanted with Si. The dielectric functions of the implanted Si subjected to a postimplant annealing were retrieved by fitting the SE spectra in the photon energy range of 1.1–4.6 eV with the Tauc–Lorentz (TL) parameterization.[7] The analysis of the dielectric functions of the implanted Si based on the evolution of the TL model parameters has provided us an insight into the possible structural changes of the implanted silicon caused by the annealing.

A Si_3N_4 thin film with thickness of about 120 nm was deposited by low-pressure chemical vapor deposition onto a 30 nm SiO_2 thin film (i.e., a stress-relief oxide layer) thermally grown on a Si (100) substrate. The Si_3N_4 film was subsequently implanted with Si ions with a dose of 3.5×10^{16} atoms/cm^2 at the energy of 30 KeV. According to the stopping and range of ion in matter calculation, the implanted Si distributes from the surface to the depth of about 75 nm following a Gaussian distribution, as shown in Fig. 1(a). The maximum volume fraction of the implanted Si is ~21%. This volume fraction peak is located at the depth of 33 nm. Afterwards, thermal annealing was carried out in nitrogen ambient at different temperatures (i.e., 800, 900, 1000, and 1100 °C) for 1 h. Transmission electron microscopy (TEM) measurement was conducted to investigate the structural properties of the Si-implanted Si_3N_4 thin films after an annealing. Si nanoparticles or nanoclusters with sizes in the order of 2 nm can be observed in the TEM images. Figure 1(b) shows a typical TEM image. The SE measurement was performed in the wavelength range of 270–1100 nm with a step of 5 nm at three incident angles (i.e., 65°, 70°, and 75°).

As shown in Fig. 1(a), the multilayer model is employed to approximate the distribution of the implanted Si. The top

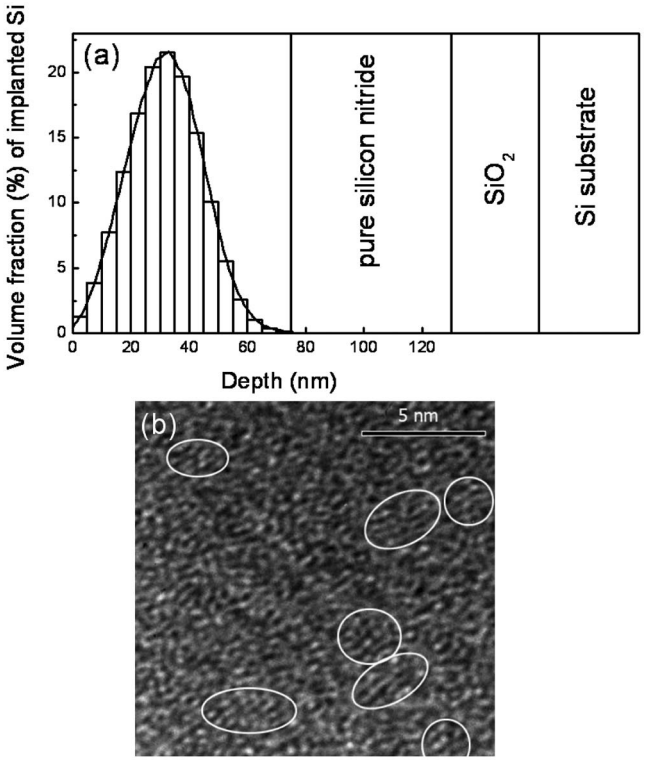

FIG. 1. (a) Multilayer model used in the SE analysis; and (b) TEM image of the Si nanoparticles or nanoclusters embedded in the Si_3N_4 thin film for the sample annealed at 1100 °C.

a)Electronic mail: cenz0001@ntu.edu.sg.
b)Electronic mail: echentp@ntu.edu.sg.

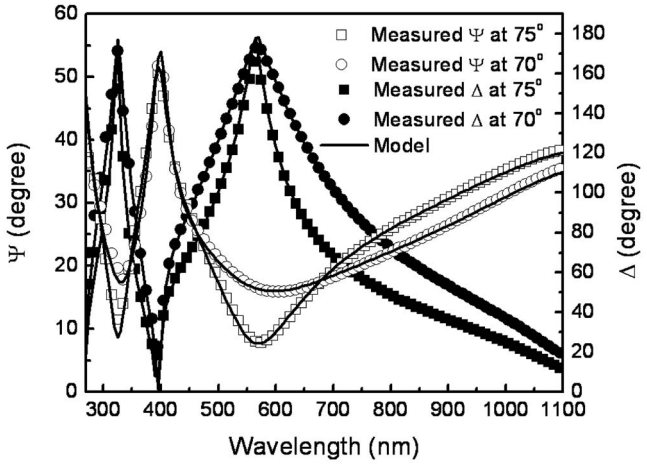

FIG. 2. Spectral fittings for the sample annealed at 1100 °C (for a clear presentation only the fittings for the incident angles of 75° and 70° are shown).

75-nm-thick layer containing the implanted Si distributed in the Si_3N_4 matrix is divided into 15 sublayers with equal thickness of 5 nm. For each of the sublayers, its dielectric function is modeled with the BEMA. The underneath remaining Si_3N_4 layer without the implanted Si is treated as a pure Si_3N_4 layer, whose dielectric functions are measured from the pure Si_3N_4 thin films of the control samples (i.e., without the Si ion implantation) by the SE method. Thus, the dielectric functions of the implanted Si can be determined through a spectral fitting to the experimental SE data by minimizing the mean square error.[5]

It has been shown that a Kramers–Kronig-consistent TL model is suitable to parameterize the dielectric functions of Si nanostructure.[8,9] Therefore, in the spectral fittings of the present study, such a TL model is used. In the TL model, the imaginary part (ε_2) of dielectric function is written as

$$\varepsilon_2(E) = \begin{cases} 0, & \text{for } 0 < E \leqslant E_g \\ \left[\dfrac{AE_0C(E-E_g)^2}{(E^2-E_0^2)^2 + C^2E^2} \cdot \dfrac{1}{E} \right], & \text{for } E > E_g, \end{cases} \quad (1)$$

where A is the amplitude of a Lorentz oscillator, E_0 is the peak transition energy, C is the broadening term, and E_g is the bandgap energy. The real part (ε_1) of dielectric function is obtained by Kramers–Kronig integration of ε_2 with a fitting constant $\varepsilon_1(\infty)$.[7] Note that $\varepsilon_1(\infty)$ was initially set to 1 in the spectral fitting. In the spectral fitting, A, E_0, C, E_g, and the thicknesses (d_{Si3N4} and d_{SiO2}) of both the Si_3N_4 layer and the SiO_2 layer are the fitting parameters. The spectral fittings were carried out for three incident angles (i.e., 65°, 70°, and 75°) simultaneously. As an example, Fig. 2 shows the spectral fittings for the sample annealed at 1100 °C. The values of the d_{Si3N4} and d_{SiO2} yielded from the fittings are 129 and 28 nm, respectively, which agree well with the TEM measurement. The swell effect due to the implanted Si can be observed by comparing d_{Si3N4} with the thickness of Si_3N_4 layer obtained from the control sample.

In order to understand the effect of annealing on the structure of the implanted Si, the evolution of the dielectric functions of the implanted Si with annealing temperature has been investigated. The real parts and imaginary parts of the dielectric functions yielded from the spectral fittings for the

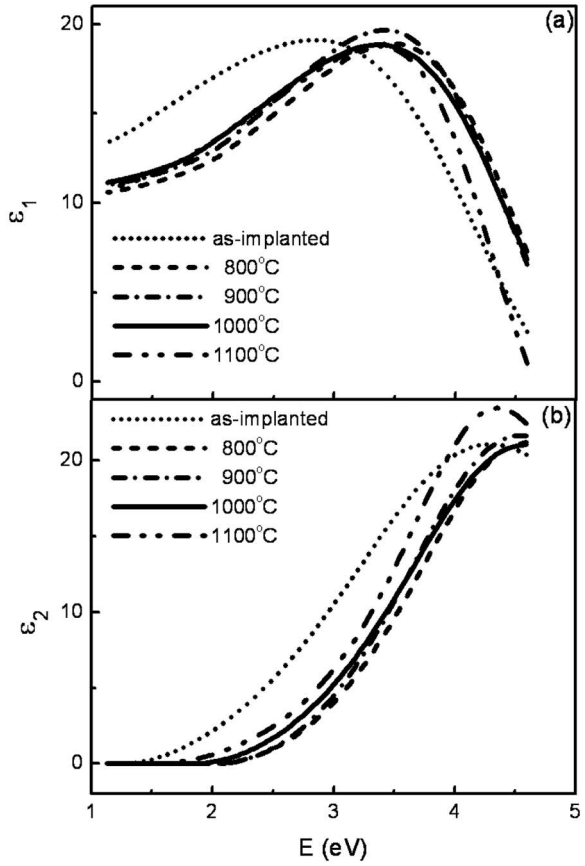

FIG. 3. Annealing effect on the dielectric functions of the implanted Si. (a) Real part (ε_1) and (b) imaginary part (ε_2) of the dielectric functions.

implanted Si of the as-implanted sample as well as the samples annealed at different temperatures are shown in Fig. 3. The obtained TL model parameters describing the dielectric functions are plotted in Fig. 4. It is observed that the dielectric functions for all the samples are generally similar. The spectral features of the dielectric functions are also similar to that of amorphous Si.[10] The broadened peak structures, particularly, the broad peaks of the as-implanted sample, suggest that the implanted Si is in amorphous or disorder state to a certain extent. The implanted Si shows a significant reduction in the dielectric functions as compared with bulk crystalline silicon (c-Si).[11] This suppression in dielectric functions is often attributed to the bandgap expansion,[4] while some argued that it results from the breaking of polarizable bonds.[12]

As can be seen in Fig. 3(b), the implanted Si exhibits a peak structure in the ε_2 spectra located near the transition energy E_2 (4.27 eV) of bulk c-Si.[11] Due to the single-term TL model employed in the spectral fittings, fine features such as the two-peak structure in the dielectric-function spectra reported in Ref. 5 cannot be revealed in the present study. However, from the second derivative of the ε_2 with respect to the photon energy,[13] one critical point is clearly identified for all the samples. The critical point is close to the transition energy E_2 of c-Si, indicating that the energy transitions related to the critical point E_2 dominate the dielectric functions of the implanted Si. No significant blueshift of E_2 is observed in this study, being consistent with the study in Ref. 14. Interestingly, the transition energy E_2 for the implanted Si without annealing redshifts slightly and the E_2 for the annealing below 1100 °C blueshifts slightly relative to the

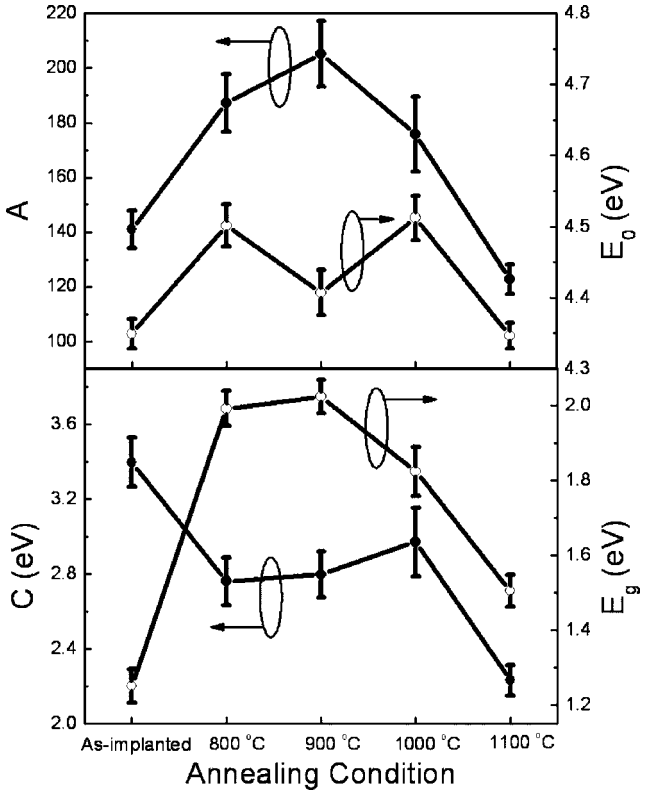

FIG. 4. Evolution of the TL parameters (i.e., A, E_0, C and E_g) with annealing temperature.

E_2 of c-Si, while the E_2 of the implanted Si annealed at 1100 °C is closest to the value of c-Si. In addition, as shown in Fig. 3(b), the ε_2 for the 1100 °C annealing is enhanced with the peak shifting toward the c-Si ε_2 main peak. These results could suggest that the annealing at 1100 °C leads to the formation of stable Si nanoclusters.

As shown in Fig. 4, the TL parameters including A, C, and E_g experience a large change after the annealing at 800 °C as compared to the situation of the as-implanted sample. They do not show a further large change for a higher annealing temperature up to 1000 °C, but they change largely again for the annealing temperature of 1100 °C. This can be accordingly translated to the changes in the structural properties of the implanted Si caused by the annealing. The decrease in the parameter C that describes the broadening of the ε_2 peak and is related to the disorder in material indicates that the annealing causes the implanted Si evolve toward an ordered state. In particular, the further reduction in the C value after the annealing at 1100 °C could suggest the formation of stable Si nanoclusters at 1100 °C. In the temperature range of up to 900 °C, the A value increases with annealing temperature, which could be due to the increase in the density of the implanted Si. However, an annealing at a higher temperature (>900 °C) leads to a decrease in the A value, which could be attributed to the phase separation between the implanted Si and the Si_3N_4 matrix as the Si–Si dipoles have a larger effective mass than the Si–N dipoles (note that A is smaller for a larger effective mass in the TL model).[7] It is interesting to note that the annealing at 800 °C causes a drastic increase in the E_g while a large decrease in the C value. This could be explained by the structural change in the implanted Si from an amorphous state to an ordered state and/or the diminishment in the absorption associated with the defects. However, the E_g decreases with annealing temperature when the temperature is higher than 900 °C, which could be due to the quantum size effect on the bandgap as a result of the Si nanocluster growth at a higher temperature. On the other hand, as can be observed in Fig. 4, annealing does not cause a large change in the peak transition energy E_0, indicating that E_0 is not very sensitive to the changes in the structural properties.

This work has been financially supported by the Ministry of Education Singapore under Project ARC No. 1/04 and by the National Research Foundation of Singapore under Project No. NRF-G-CRP 2007-01.

[1]B. H. Kim, C. H. Cho, T. W. Kim, N. M. Parka, G. Y. Sung, and S. J. Park, Appl. Phys. Lett. **86**, 091908 (2005).
[2]L. Dal Negro, J. H. Yi, L. C. Kimerling, S. Hamel, A. Williamson, and G. Galli, Appl. Phys. Lett. **88**, 183103 (2006).
[3]R. Huang, K. J. Chen, H. P. Dong, D. Q. Wang, H. L. Ding, W. Li, J. Xu, Z. Y. Ma, and L. Xu, Appl. Phys. Lett. **91**, 111104 (2007).
[4]T. P. Chen, Y. Liu, M. S. Tse, O. K. Tan, P. F. Ho, K. Y. Liu, D. Gui, and A. L. K. Tan, Phys. Rev. B **68**, 153301 (2003).
[5]L. Ding, T. P. Chen, Y. Liu, C. Y. Ng, and S. Fung, Phys. Rev. B **72**, 125419 (2005).
[6]D. A. G. Bruggeman, Ann. Phys. **24**, 636 (1935).
[7]G. E. Jellison and F. A. Modine, Appl. Phys. Lett. **69**, 371 (1996).
[8]D. Amans, S. Callard, A. Gagnaire, J. Joseph, G. Ledoux, and F. Huisken, J. Appl. Phys. **93**, 4173 (2003).
[9]M. Losurdo, M. M. Giangregorio, P. Capezzuto, G. Bruno, M. F. Cerqueira, E. Alves, and M. Stepikhova, Appl. Phys. Lett. **82**, 2993 (2003).
[10]*Handbook of Optical Constants of Solids*, edited by E. D. Palik (Academic, New York, 1985).
[11]C. M. Herzinger, B. Johs, W. A. McGahan, J. A. Wollam, and W. Paulson, J. Appl. Phys. **83**, 3323 (1998).
[12]C. Q. Sun, Prog. Solid State Chem. **35**, 1 (2007).
[13]B. Gallas and J. Rivory, J. Appl. Phys. **94**, 2248 (2003).
[14]B. Gallas, I. Stenger, C. C. Kao, S. Fisson, G. Vuye, and J. Rivory, Phys. Rev. B **72**, 155319 (2005).